Supplementary Discussion

Auto-correlation of retinal ganglion cell mosaics shows hexagonal structure

Wässle and colleagues first observed that the local structure of cell mosaics was approximately hexagonal[1], as the histogram of the angular difference of all neighbors to a reference cell within some distance showed a mode at 60deg. Their analysis was based on the location of the cell bodies (not the receptive fields). However, the same conclusion holds true if one uses the actual centers of the receptive field themselves, obtained by simultaneously mapping them by means of electrode arrays[2]. **Supplementary Fig 1** shows a (smoothed) auto-correlation of a sample mosaic of receptive field centers shown on the left. These data are from one of the reconstructed mosaics in Gauthier et al (2009). The center peak at the origin was removed to ease visualization. It can be seen the structure of the secondary peaks is clearly hexagonal. Further, one can also detect the presence of additional peaks beyond the secondary peaks, indicating the spatial scale over which the RGC mosaic is hexagonal extends farther than its immediate neighborhood. The spatial scale over which such hexagonal structure is present is now a matter of additional research.

Auto-correlation function in individual maps

As already mentioned in the text, regions of interest (ROI) in the experimental maps were selected by avoiding areas that were too close to the V1/V2 boundary and having an intermediate size. For each individual we choose between 2 to 4 non-overlapping ROIs (this choice was limited by the field of view of the camera and the size of the ROI). After calculating the auto-correlation for each individual ROI (three sample calculations are shown in **Supplementary Fig 2**), the result is scaled and rotated so that the dominant secondary peak mapped to the (1,0) point in the plane. The transformed images were then averaged to yield the

average auto-correlation for that individual animal (**Supplementary Fig 2**, right panel). These are the images, along with their local maxima, that are presented in **Fig 3a**.

Statistical significance of secondary peaks in the auto-correlation function

To verify if the secondary peaks in our calculations are statistically significant, we calculated the probability they could have resulted by chance from control maps the power spectrum of which were isotropic (see **Supplementary Figure 3** for a flow chart of this calculation). This was done by first generating an isotropic Fourier spectrum that matched the marginal radial spectrum from the measured map. We then assigned random phases to each coefficient and iterated a number of times the following steps:

1. Perform an inverse Fourier transform, resulting in a complex image
2. Normalize each pixel value (a complex number) to have a magnitude of one
3. Take a 2D FFT of the result
4. Enforce amplitude spectrum to equal that of the isotropic control.

After a number of iterations (=1000), the algorithm produces an orientation map where the spectrum satisfies the constrained imposed by the isotropic spectrum and where every pixel in the complex image has a magnitude of one. The phase of this image represents a control orientation map. We generated a family of N=500 such control images.

Next, we calculated a set (M=500) of average auto-correlation images by randomly sampling (without replacement) K of them, where K was the actual number of ROIs used in each case (2 to 4), and averaging them after alignment with the dominant peak. From this set of auto-correlation control images we can calculate the probability that each of the local maxima observed in the average auto-correlation could have resulted by chance under the null hypothesis that the map was isotropic. This is done by looking at the values attained at the same location of the peak in the family of control average auto-correlations. Then we ask how many of the control values exceed the one actually measured and divide it by the their total number to obtain the p-value.

Example of mosaic and map with realistic levels of noise

An example of an interference pattern and the resulting orientation map with realistic levels of noise is shown in **Supplementary Fig 4**. Under this conditions it is difficult under visual inspection to observe a clear interference pattern, but the robustness of the structured input becomes evident in clustering of dipoles with similar orientation in the orientation map.

Relationship between mosaic parameters and the period of orientation columns

What scaling factors are necessary to match the period of the map observed in the retina to the observed periodicity in the cortex?

The following estimates are based on the published reconstructions of RGC receptive fields of *M. fascicularis* [3]. By computing the mean and standard deviation of nearest neighbor distances for each class of cells (**Fig 4**), and by assuming the mosaics arise from a noisy hexagonal lattice, one can estimate the magnitude of the positional noise and the grid spacing of the lattice.

Using the magnocellular mosaic in Figure 2 of Gauthier et al. (2009), we obtain $d_{ON} = 156\mu m$, $d_{OFF} = 142\mu m$. In both cases, independent estimates of the noise expressed as a fraction of the grid spacing was $\sigma = 0.12 \times d$. Thus, in terms of the parameters used in Figure 1 this implies that $\alpha = 0.105$ and $d = 142\mu m$.

In the primate eye, the nonlinear relationships between retinal eccentricity (in mmr) and visual angle (in deg) is given by, $A = 0.1 + 4.21E + 0.038E^2$ [4] (we will adopt mmr to mean "millimetres on the retina" while mmc will denote "millimetres on the cortex"). The reconstruction of this particular mosaic originates from a 9 mmr eccentric location,

corresponding to 41° of visual angle. At this eccentricity, the cortical magnification factor is approximately 0.146 mmc/deg [5]. From the above formula, we also obtain $dA/dE = 4.21 + 0.076E$ (deg/mmr), which evaluated at 9mmr gives 4.9 deg/mmr. This means that at this retinal eccentricity we obtain a factor of $4.9\,\text{deg/ mmr} \times 0.146\text{mmc / deg} = 0.715\text{mmc/mmr}$.

The period of the orientation map in *M. fascicularis* is approximately 0.750mmc[6-7], which translates to a period on the retina of 1.05mmr. We conclude that if the orientation map were to be set up by the mosaics of magnocellular RGCs we would need a scale factor of $S = 1.05\text{mmr} / 0.142\text{mmr} = 7.4$. Finally, having $S = 7.4$ and $\alpha = 0.1$, we estimate the relative rotation between the arrays to be $\theta = 6\,\text{deg}$ (from the equation provided in the main text).

Similar estimates can be performed for the parvocellular mosaics. Our estimates here result in $d_{ON} = 106\mu\text{m}$, $d_{OFF} = 101\mu\text{m}$ and $\sigma = 0.13 \times d$ for both mosaics. This generates values of $\alpha = 0.05$ and $d = 101\mu\text{m}$. Thus, the estimated scaling factor would be $S = 1.05\text{mmr} / 0.101\text{mmr} = 10.4$, from which we estimate a relative rotation of $\theta = 5\,\text{deg}$.

These analyses predict that there RGC mosaics for ON- and OFF-center cells should not be statistically independent. We should be able to measure a consistent angular difference between the two. One way to do this is to compute the auto-correlations for both ON- and OFF-center mosaics as shown in **Supplementary Figure 1** and see if the hexagonal structures have different angles. Such studies are currently under way.

Supplementary Figure Legends

Supplementary Fig 1. Autocorrelation of the *receptive field* locations mapped by multi-electrode array shows clear hexagonal structure (red hues correspond to higher correlation values). Thus the hexagonal structure of RGC mosaics is reflected both in the cell body locations as well as in the receptive field locations.

Supplementary Fig 2. Calculation of auto-correlation function in a single individual. A number of non-overlapping ROIs (three exemplified in this case) are obtained from the orientation map. Their auto-correlations are then computed and the largest local maxima identified (solid dots). Each auto-correlation image is then rotated and scaled so as to bring the dominant peak to the point (0,1). The average of these normalized functions results in the average auto-correlation shown on the right. Scale bars represents the map period in each case.

Supplementary Fig 3. Statistical significance of local peaks in auto-correlation functions. Orientation control maps are generated by a procedure that ensures they have the same radial Fourier amplitude spectrum as the measured ones. Their auto-correlation functions serve as a family that represent control samples for the maps in the ROIs. We then calculate what would be the family of auto-correlations we can expect given K ROIs, where K is the actual number of ROIs we used to calculate the auto-correlation function in each case. From this family we can obtain the distribution of amplitudes at any location in the map and use their values to estimate the probability that the magnitude of the local peak we measure could have resulted by chance. As the number of functions we generated was M=500 we can only assess significance down to a level of $p<0.002$, which was attained in all cases. Thus, the magnitude of the local peaks seen in the data are very unlikely to have resulted by chance.

Supplementary Fig 4. Example of mosaics and orientation map perturbed by a realistic level of noise. Scale bar 1mm of cortical space. Format is the same as **Fig 1d**.

References

1. Wassle, H., Boycott, B.B. & Illing, R.B. Morphology and Mosaic of on-Beta and Off-Beta Cells in the Cat Retina and Some Functional Considerations. *Proceedings of the Royal Society of London Series B-Biological Sciences* **212**, 177-& (1981).
2. Gauthier, J.L., *et al.* Uniform signal redundancy of parasol and midget ganglion cells in primate retina. *J Neurosci* **29**, 4675-4680 (2009).
3. Gauthier, J.L., *et al.* Receptive fields in primate retina are coordinated to sample visual space more uniformly. *PLoS Biol* **7**, e1000063 (2009).
4. Dacey, D.M. & Petersen, M.R. Dendritic field size and morphology of midget and parasol ganglion cells of the human retina. *Proc Natl Acad Sci U S A* **89**, 9666-9670 (1992).
5. Vanessen, D.C., Newsome, W.T. & Maunsell, J.H.R. The Visual-Field Representation in Striate Cortex of the Macaque Monkey - Asymmetries, Anisotropies, and Individual Variability. *Vision Research* **24**, 429-448 (1984).
6. Obermayer, K. & Blasdel, G.G. Geometry of Orientation and Ocular Dominance Columns in Monkey Striate Cortex. *Journal of Neuroscience* **13**, 4114-4129 (1993).
7. Nauhaus, I., Benucci, A., Carandini, M. & Ringach, D.L. Neuronal selectivity and local map structure in visual cortex. *Neuron* **57**, 673-679 (2008).

Sample OFF-center RGC mosaic

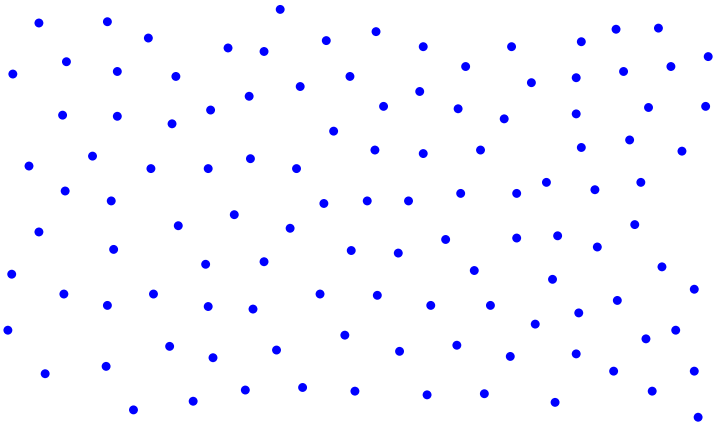

Auto-correlation
with center peak suppressed

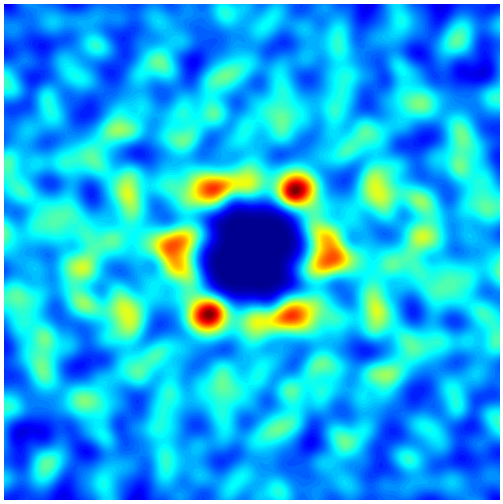

Supplementary Fig 1

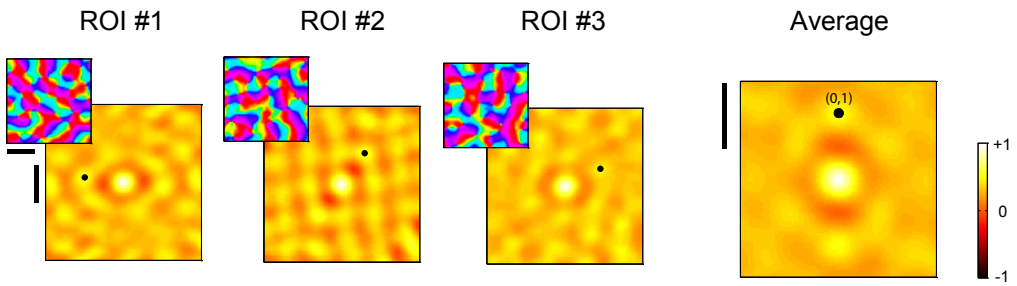

Supplementary Fig 2

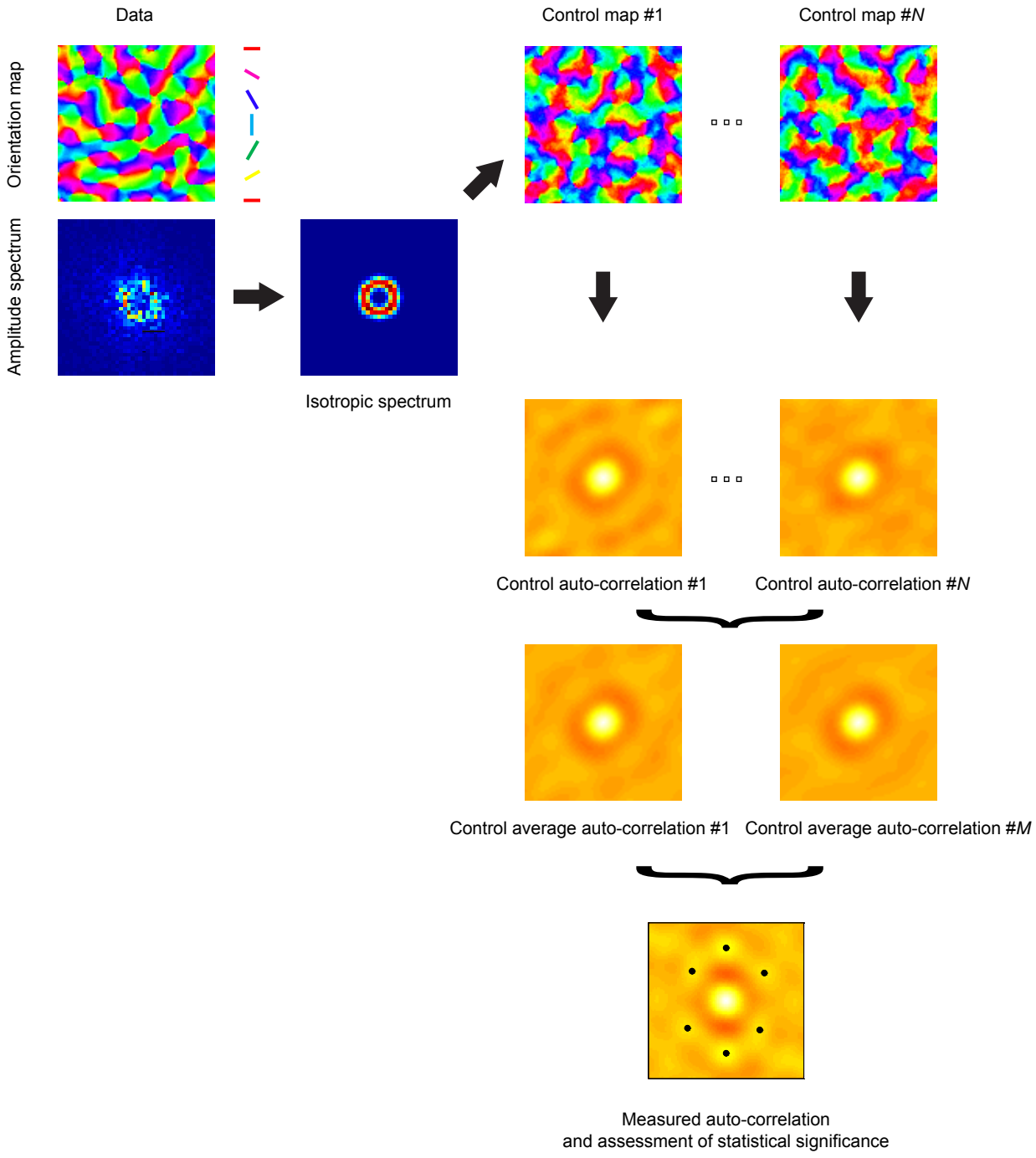

Supplementary Fig 3

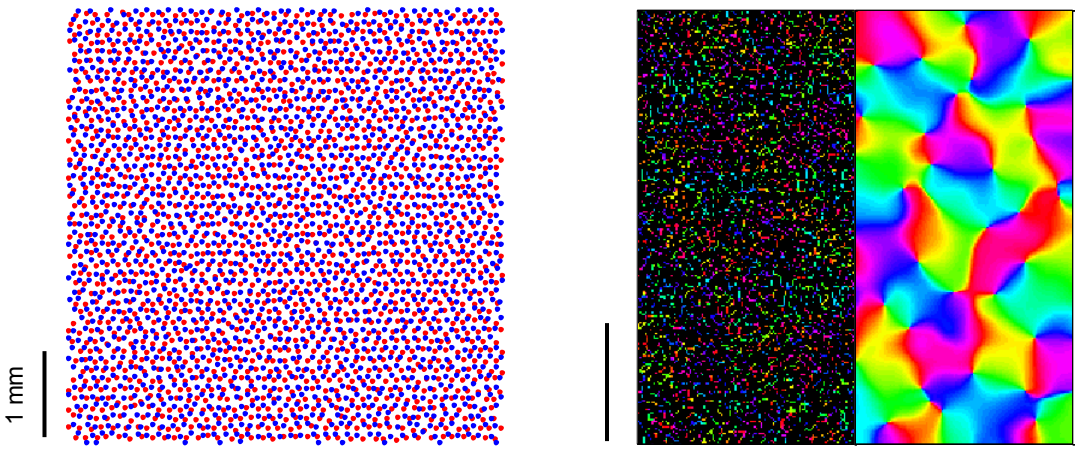

Supplemental Figure 4